Ex vivo Study of Prostate Cancer Localization Using Rolling Mechanical Imaging towards Minimally Invasive Surgery

Jichun Li[1, 5, 6]*, **Hongbin Liu**[1], **Matthew Brown**[2], **Pardeep Kumar**[2, 7], **Ben Challacombe**[2, 7], **Ashish Chandra**[3], **Giles Rottenberg**[4], **Lakmal Seneviratne**[1, 9], **Kaspar Althoefer**[1, 8], **Prokar Dasgupta**[2, 7]

[1] Centre for Robotics Research, Department of Informatics, King's College London, UK.

[2] Department of Urology, Guy's and St Thomas' Hospital NHS Foundation Trust, London, UK

[3] Department of Histopathology, Guy's and St. Thomas' Hospitals, London UK

[4] Department of Radiology, Guy's and St. Thomas' Hospitals, London UK

[5] School of Engineering and Computing Sciences, Durham University, UK

[6] School of Electrical and Electronic Engineering, Newcastle University, UK

[7] MRC Centre for Transplantation, NIHR Biomedical Research Centre, King's Health Partners, Guy's Hospital, London, UK

[8] Centre for Advanced Robotics @ Queen Mary (ARQ), Faculty of Science and Engineering, Queen Mary University of London, London, UK.

[9] Khalifa University Robotics Institute, Khalifa University, Abu Dhabi, UAE.

* Corresponding author: jichun.li@newcastle.ac.uk

Abstract

Rolling mechanical imaging (RMI) is a novel technique towards the detection and quantification of malignant tissue in locations that are inaccessible to palpation during robotic minimally invasive surgery (MIS); the approach is shown to achieve results of higher precision than is possible using the human hand. Using a passive robotic manipulator, a lightweight and force sensitive wheeled probe is driven across the surface of tissue samples to collect continuous measurements of wheel-tissue dynamics. A color-coded map is then generated to visualize the stiffness distribution within the internal tissue structure. Having developed the RMI device in-house, we aim to compare the accuracy of this technique to commonly used methods of localizing prostate cancer in current practice: digital rectal exam (DRE), magnetic resonance imaging (MRI) and transrectal ultrasound (TRUS) biopsy. Final histology is the gold standard used for comparison. A total of 126 sites from 21 robotic-assisted radical prostatectomy specimens were examined. Analysis was performed for sensitivity, specificity, accuracy, and predictive value across all patient risk profiles (defined by PSA, Gleason score and pathological score). Of all techniques, pre-operative biopsy had the highest sensitivity (76.2%) and accuracy (64.3%) in the localization of tumor in the final specimen. However, RMI had a higher sensitivity (44.4%) and accuracy (57.9%) than both DRE (38.1% and 52.4% respectively) and MRI (33.3% and 57.9% respectively). These findings suggest a role for RMI towards MIS, where haptic feedback is lacking. While our approach has focused on urological tumors, RMI has potential applicability to other extirpative oncological procedures and to diagnostics (e.g., breast cancer screening).

Keywords: Rolling mechanical imaging, robotic minimally invasive surgery, wheeled probe

1. Introduction

Prostate cancer [1] is the most common male malignancy and an average of 1 in 8 men will be diagnosed with prostate cancer during their lifetime. Treatment of prostate cancer by surgical extirpation (radical prostatectomy) or by tissue destruction in situ (e.g., radiotherapy or brachytherapy) frequently compromise potency and urinary control. The key tenet of preserving functional outcomes in prostate surgery is to effectively treat the prostate tumor, but spare adjacent tissues involved in urinary control (e.g., bladder neck and urethral length) as well as erectile function (cavernous nerves). This principle means that prostate surgeons walk a continual tightrope between removing adequate tissue to treat the cancer (the tumor plus a margin) and avoiding unnecessary resection of tissue important to functional outcomes.

For centuries, surgeons have used texture and firmness to discriminate between benign and malignant tissue when dissecting at operation. In the modern era of prostate cancer surgery, a surgeon subtly modifies dissection planes in real time during an operation, combining subjective haptic data with visual cues and knowledge of pre-operative assessments (including imaging and statistical models). The advent of robotic surgery (such as the da Vinci^{TM} Surgical System has provided a high definition stereoscopic vision, tremor free scalable manipulation with high degrees of freedom at the operating fulcrum, and an ergonomic operating position [2,3]. This significantly improves the ease at which prostate cancer surgery (radical prostatectomy) can be performed. However, robotic surgery throws down a new challenge, because it deprives surgeons of haptic feedback and therefore tissue stiffness assessment afforded by their fingers or dissection instruments. Therefore, dissection planes and in particular, bladder neck sparing or nerve sparing increments can be decided only by pre-operative assessments about tumor stage and visual cues [4].

It is possible that the loss of haptic feedback is one reason why robotic surgery has failed to deliver convincingly (at least to date) significant improvements in functional outcomes relative to open or conventional laparoscopic surgery. Furthermore, given tumor localization is critical to surgical precision and ultimately patient outcomes, new techniques to replace the loss of haptic feedback are paramount. Integration of MRI tumor localization into operative planning has been a recent advancement, but real time MRI remains impractical due to the physical size of the scanner and the expense involved. Early reports showed that only 60% of prostate cancer lesions which are greater than 5mm could be detected [5]. MRI is useful for predicting tumor size of cancer foci greater than 10 mm in diameter [6]. But several studies also indicated that the external coil was not reliable enough for the detection of tumor volume [7, 8]. In recent years, endorectal MRI (erMRI) has obtained improved results, reportedly achieving an accuracy of up to 82% in the prospective evaluation of patients previously diagnosed of prostate cancers [9]. Despite these technological advances, the use of MRI for the localization of prostate cancer is still controversial. Furthermore, it is difficult to register pre-operative imaging to intraoperative tumor locations in real time, due to the deformability and movement of the prostate during surgery.

Transrectal ultrasound (TRUS) was the first imaging technique to be used for prostate tumor localization [10] in the planning stage of prostate cancer surgery, and in real-time during radical prostatectomy. Prostate cancers typically appear as hypoechoic lesions on TRUS, but unfortunately, 80% of hypoechoic lesions found on TRUS are not cancer [11]. Furthermore, 30% of prostate cancers are iso-echoic on TRUS and will not be detected [12]. Thus, the utility of TRUS in localization of prostate cancer is limited. A newer development in ultrasound technology is elastography. The principle of ultrasonic elastography is similar to RMI, in that soft tissues exhibit greater deformation than stiff tissue. In the case of ultrasound, this difference in deformation can

be detected by a speckle map of backscatter, which is converted to an elastogram as a qualitative readout of tissue stiffness [13]. Although some efforts of adapting elastography into laparoscopic surgery has been reported [14], however, numerous limitations still remain for its adoption: the required ultrasound transducers are difficult to miniaturize, the readout requires a deformation force to be applied by the operator (which can be variable from clinician to clinician) and the more distant tissue from the probe is less reliably assessed [15]. Thus elastography for large prostates and the prostatic base can be difficult to interpret and unfortunately, when it comes the preservation of functional tissue, it is exactly these positions wherein knowledge of tumor location can be extremely important. Additionally, TRUS-elastography has not been applied in real time during surgery, and continues to be marketed only as a diagnostic adjunct.

Here we report a new modality in development: Rolling Mechanical Imaging (RMI) using a passive robotic manipulator. RMI is a novel approach using a force sensitive wheeled probe [16-22], which overcomes some of the limitations of the competing elastography technology. In particular, RMI provides a uniform deforming force (not operator dependent) and a readout of tissue elasticity or stiffness that is objective, quantitative, and can be acquired in real-time. Moreover, instead of performing a series of discrete uniaxial measurements [23], the probe allows for the continuous measurement of the tool-tissue interaction dynamics as it rolls over the surface of the tissue. Rapid surface coverage and enhanced sensitivity to tissue irregularities can hence be achieved. By fusing the tissue reaction forces measured along trajectories, the variations in mechanical tissue properties can be mapped to demonstrate the geometrical stiffness distribution of the examined tissue. The goal of this study is to assess the accuracy of RMI on freshly excised and extracted prostates under ex vivo situation for localization of cancer and compare it with the accuracy of MRI, DRE and TRUS biopsy.

2. Materials and Methods

2.1 Human specimen preparation

The study was given full ethical approval by NHS Research Ethics Committee to be conducted at the Departments of Urology, Radiology and Histopathology, Guy's and St Thomas' Hospital and the patients provided written informed consent allowing the post-operative examination. All patients had undergone radical prostatectomy to treat prostate cancer. The mean age of patients was 64.2±5.2 years. Patients with clinically insignificant small cancers (<0.5mL) were excluded in the sample. In total, 21 prostate specimens were tested for analysis. The mean PSA level was 8.5±3.4 ng/mL. The prostate cancer specimens were classified according to final pathologic findings. The stage of the prostate cancer obtained with this system was T2b in 5 patients; T2c in 6 patients; T3a in 10 patients. The specimen obtained contains various sizes of cancer tumors ranging from 5mm - 20mm in diameter.

2.2 Rolling mechanical imaging Device

A device for performing rolling mechanical imaging (RMI) was developed as shown in Fig.1. This device contains a haptic console (Phantom OmniTM) which providing six degrees of freedom position sensing. The haptic console is attached to a specially designed wheeled probe head integrated with a 6-DOF ATI Nano17 Force/Torque sensor (calibration SI-25-0.25, resolution 0.003 N with 16-bit DAQ), which can roll over a soft tissue while measuring the tissue stiffness, Fig.1. The Phantom Omni is a passive robotic device which is moved into different configurations (positions and orientations) by hand wrist movements, with a nominal positional resolution of 0.055 mm. Three potentiometers and three encoders were used to read the outputs
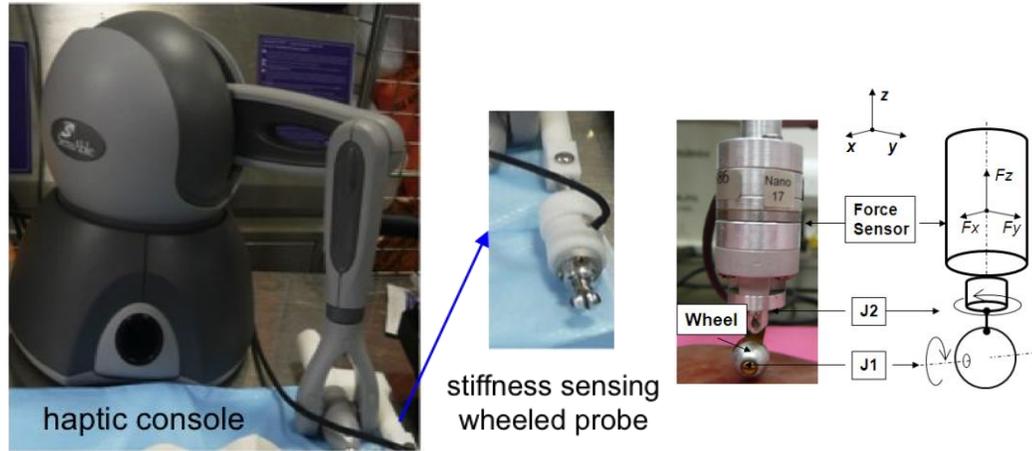
Fig.1 Rolling Mechanical Imaging (RMI) device. Device consists of haptic console and stiffness sensing wheeled probe. The haptic console, Phantom Omni, is a passive robotic device with position and orientation of the probe being set by hand wrist movements, with a nominal positional resolution of 0.055 mm. The force sensor is a 6-DOF ATI Nano17 Force/Torque sensor (calibration SI-25-0.25, resolution 0.003 N with 16-bit DAQ).

of the device - six variable angles – three joint angles for translation and three gimbal angles for rotation. The necessary probe trajectories can be set by programming based on dynamic link libraries provided. The protocol for measuring stiffness of a prostate specimen is described as follows: Firstly, the three-dimensional (3D) surface registration was carried out by scanning the prostate specimen using the proposed apparatus. The 3D surface model representing dimensions of the measured specimen was created using MATLAB software package. The scanning trajectories then were defined and programed with a scanning resolution of ±0.5mm, Fig. 2. Secondly, the probe rolled again over the specimen for the second scanning with an indentation depth of 3 mm following the programmed scanning trajectories. The average scanning speed is set to 10 mm/s. The mechanical properties were acquired from the wheeled probe head combined with the National Instruments LabView 8.0 software package and associated PCI Data Acquisition Card (NI PCI 6034E, which is a 16-bit DAQ card) during rolling indentation. The developed RMI device integrates the rolling trajectory of the wheeled probe head with the stiffness measurements to

generate a three-dimensional stiffness image of the examined prostate tissue as shown in Fig. 3. Since the image indicates the stiffness distribution within the soft tissue, the location of the tumors can be identified.

In this study, the prostate specimen, which the probe rolled over were assumed to have the following properties: the normal tissue of the organ were assumed isotropic, homogenous, and incompressible. In addition, the normal tissues were assumed to be linear elastic - biological tissues is said to exhibit linear elasticity with small deformation [26].
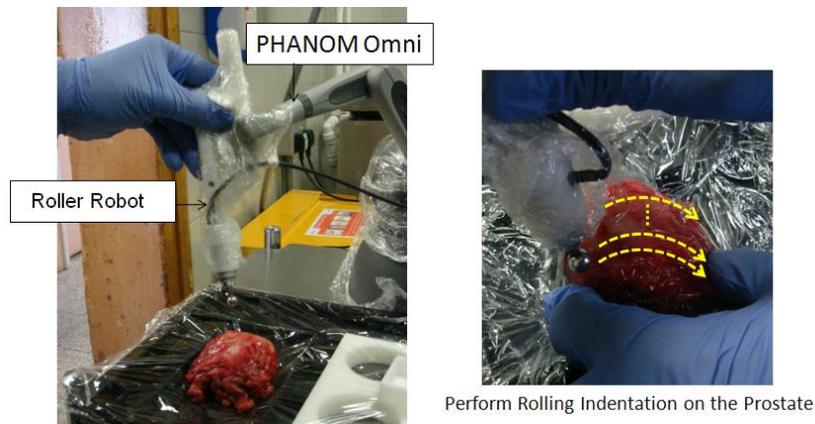

Fig.2 Application of RMI to a prostate specimen conducting rolling indentation following pre-defined trajectories. The prostate laid on a flat and hard surface during the application of the sensor probe.
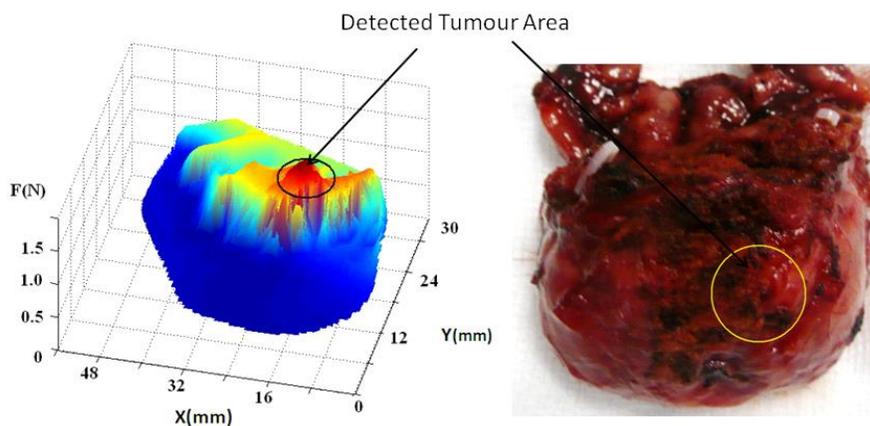

Fig.3 Three dimensional stiffness image of prostate specimen. High stiffness depicted as yellow and red. Tumor location correlated with stiffness, as shown.

3. Experiments

During the experiments, the trained operator who performed the experiments was blind to the clinical data. Ex vivo tests using the RMI device were carried out on the extracted human prostates within 60 minutes after extraction of the specimen in the operating room. Each test was conducted 3 times. Ex vivo tests of RMI were performed by several trained researchers. The clinical experts determined the divided sites of specimens. Biopsy results provide information about tumor location for surgeons during operation. The test is performed on six prostate segments, therefore, for the comparative study it was necessary to divide the acquired stiffness map into six parts. Each segment contained information about tissue condition – either it was healthy tissue segment or it contained a tumor, Fig. 4. After completing rolling indentation tests, the specimens were sent to the pathology department for histological examination at Guy's and St Thomas' Hospitals, London. The specimens were prepared by fixing them in formalin and were then examined by an index pathologist using an optical microscope. The pathologist was blind to the results of RMI and documented the location and size of the cancer tissues for all specimens. A total of 126 areas were recorded for comparison with clinical results on the 21 specimens. Fig. 5 shows a comparative result of RMI with clinical reporting proformas on a selected prostate.
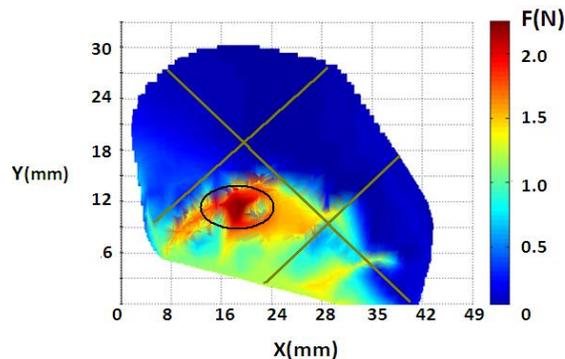

Fig.4 Tissue stiffness map is subdivided into six segments, with areas of low stiffness shown blue, intermediate denoted as yellow, and high stiffness depicted as red.
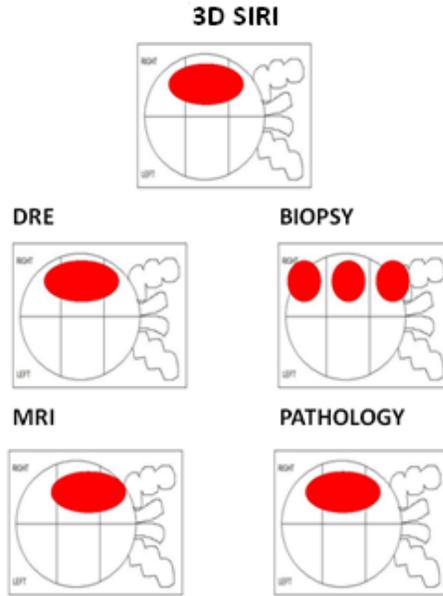
Fig. 5 Representative patient. Location of tumor on pathology, biopsy, MRI, DRE and 3D SIRI depicted.

4. Results

In total 126 sites of 21 prostates from male patients undergoing robot-assisted radical prostatectomy were examined. The generated RMI maps were correlated with digital rectal examination, MRI and TRUS biopsy results.

The *t-test* [24-26] examine whether the mean of two groups are statistically different from each other. In order to establish differences among the different methods, the paired *t-test* was used to determine differences between MRI and other methods. A 2×2 Chi-square Test (Four-fold Contingency Table), which is the most commonly used for comparing new diagnosis method with the "Gold standard" test. For prostate cancer diagnosis, final histology is always the "Gold standard" test. Thus, in this paper, the final histology was used as ground truth and the accuracy was calculated from the 2×2 confusion matrix.

We denote True Positive (TP) as correctly identified, True Negative (TN) as correctly rejected, False Positive (FP) as incorrectly identified, False Negative (FN) as incorrectly rejected, the

sensitivity, specificity, the precision or positive predictive value (PPV), the negative predictive value (NPV) and the accuracy are defined as [24, 25]:

$$Sensitivity = \frac{TP}{TP+FN}$$
$$Specificity = \frac{TN}{TN+FP}$$
$$PPV = \frac{TP}{TP+FP} \qquad (1)$$
$$NPV = \frac{TN}{TN+FN}$$
$$Accuracy = \frac{TP+TN}{TP+FP+FN+TN}$$

Wilson score intervals [26], which were calculated for those statistical measures at a 95% confidence level, are defined using the following formula:

$$\frac{1}{1+\frac{z^2}{n}}\left[\hat{p} + \frac{z^2}{2n} \pm z\sqrt{\frac{\hat{p}(1-\hat{p})}{n} + \frac{z^2}{4n^2}}\right] \qquad (2)$$

where n is the sample size, $\hat{p}$ is the proportion of successes estimated from the statistical sample and z is the 1-α/2 percentile of a standard normal distribution where α is the error percentile. Here, the confidence level is 95%, the error α is 5%. This interval has good properties even for a small number of trials so it is suitable for the chosen sample size of 126.

Correlation was performed using a visual scale proforma by researchers blinded to the purpose of the study. Fig. 6 shows a three-dimensional color-code which indicates stiffness distribution and tumor locations of a human prostate. The tumor showed up as distinctly red colored areas (higher stiffness). The summary of the statistical analysis of the results is shown in Table 1. When RMI was compared to histology as the gold standard, it exhibited 44.4% sensitivity and 71.4% specificity for the detection of prostate tumors. This equates to a 56.3% NPV, 60.9% positive predictive value and 57.9% accuracy. Interestingly, the performance of RMI in the detection of tumor was not affected by the patient's risk profile (as denoted by Gleason score, PSA,

pathological stage) as sensitivity, specificity, NPV, PPV and accuracy were comparable across all patient risk strata.

Table 1. The Statistical Analysis of the Tumor Localization Using RMI, DRE, MRI and TRUS

Methods	RMI	DRE	MRI	TRUS
	TP=28 FP=18 FN=35 TN=45	TP=24 FP=21 FN=39 TN=42	TP=21 FP=11 FN=42 TN=52	TP=48 FP=30 FN=15 TN=33
Sensitivity	44.4%	38.1%	33.3%	76.2%
Specificity	71.4%	66.7%	82.5%	52.4%
NPV	56.3%	51.9%	55.3%	68.8%
PPV	60.9%	53.3%	63.6%	61.5%
Accuracy	57.9%	52.4%	57.9%	64.3%

4.1 Comparing the accuracy of RMI and DRE

DRE was 38.1% sensitive for prostate tumor overall and had 66.7% specificity, 51.9% NPV, 53.3% positive predictive value and 52.4% accuracy. Hence, the localization of prostate cancer with RMI was superior to the human hand in all of the experiments. Therefore, the addition of RMI to DRE during intraoperative assessment of tumor could result in a 5.5% increase in accuracy, a 6.4% increase in sensitivity, a 4.7% increase in specificity, a 4.4% increase in NPV and a 7.6% increase in PPV.

4.2 Comparing the accuracy of RMI and MRI

Compared to histology, MRI had 33.3% sensitivity, 82.5% specificity, 55.3% NPV, 63.6% PPV and 57.9% accuracy. RMI therefore performed better than MRI with respect to sensitivity (11.1% increase). However, RMI was 11.1% less specific for prostate cancer detection overall when compared to MRI. The NPV of RMI is 1% better than MRI, PPV of RMI decreases 2.7% compared to MRI. The accuracy was the same between RMI and MRI. In some case, the RMI can detect tumors which are invisible to MRI, Fig.6.

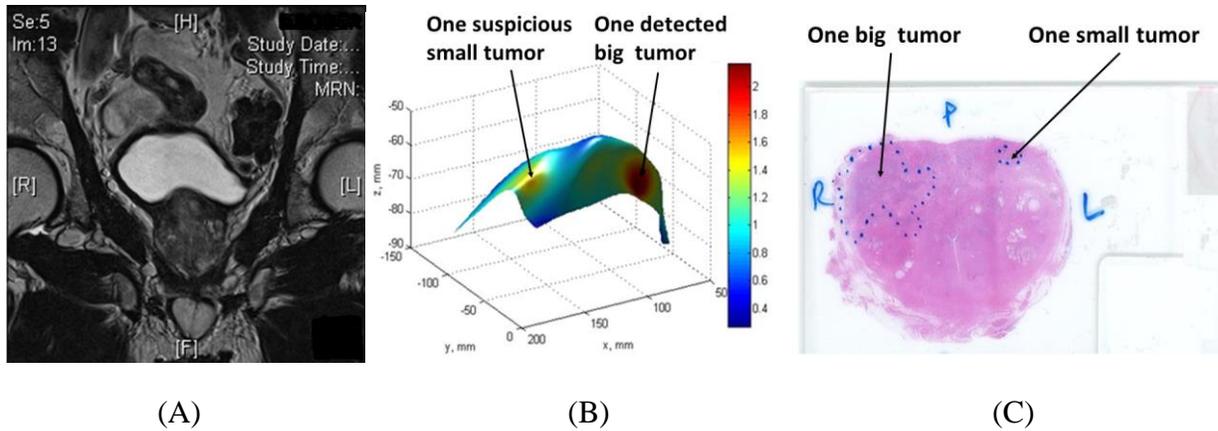<div align="center">(A)   (B)   (C)</div>

Fig. 6. Patient with tumor which was detected by RMI (B) and pathology (C), but was invisible on MRI (A). This case clearly showed that RMI was able to identify the big tumor and to some extent the small tumor as found out by the pathology. So RMI is as good as pathology here.
(A) MRI results shows that there is no tumor. (B) RMI shows that there is one big tumor and one suspicious small tumor. (C) Pathology examination shows that there is one big tumor and one small tumor at the same locations.

4.3 Comparing the accuracy of RMI and Pre-operative TRUS biopsy

Pre-operative TRUS biopsy had 76.2% sensitivity, 52.4% specificity, 68.8% NPV, 61.5% PPV and 64.3% accuracy. Therefore TRUS biopsy performed considerably better than RMI with respect to sensitivity (76.2% versus 44.4%) and NPV (68.8%. versus 56.3%). However, RMI had 19% greater specificity. In all other experiments, biopsy and RMI produced very similar results.

5. Discussion

Real time imaging for tumor localization has the potential to significantly improve both functional and oncological outcomes for robot assisted prostate cancer surgery. RMI has demonstrable utility given its similar diagnostic capabilities to MRI (the latter being prohibitive in terms of expense and physical scale within the operating theatre environment). MRI had higher specificity than RMI (82.5% versus 71.4%) but RMI had an 11.1% higher sensitivity. Indeed, in Fig. 6, we demonstrate a case where a patient had a tumor detectable by RMI and pathology but this lesion was invisible on MRI. As mentioned in the introduction section, MRI is useful for predicting tumor size of cancer foci greater than 10 mm in diameter [4]. Due to the higher resolution (the positional

resolution of the Phantom OmniTM is 0.055mm; the force resolution is 0.003N; and, the scanning resolution is ±0.5mm), the probe is sensitive to the existence of a small tumor buried near the surface of the organ. In this study, a T2b stage cancer tumor buried within 3 mm below the surface and with size of about 6mm in diameter could be detected.

RMI had a lower positive predictive value, accuracy and sensitivity relative to TRUS biopsy, but RMI is not meant to replace pre-operative TRUS biopsy. Rather RMI was intended to aid intraoperative decision-making once prostate cancer has been diagnosed. However, it might be possible to utilize RMI in the diagnostic setting to help map likely locations of prostate cancer that might be targeted for biopsy – but we have yet to explore this potential application.

In fact, current screening for prostate cancer is a combination of DRE and PSA to select patients for biopsy. In this study, RMI has a greater accuracy than DRE for all measures of prostate tumor localization, which could be explained by the high force resolution (0.003N) of the probe. Given RMI uses a small sensor head, it might be adaptable into a rectal probe and this may be a useful adjunct in selecting patients for prostate biopsy in the primary care setting. An inherent limitation of this technology is the inability to detect small tumors located deep within the prostate, although technical advances might allow better detection in the future. This suggests that a sensitivity threshold of the probe does exist. This threshold is a function of the tumor size, the buried depth of the tumor, the rolling indentation depth, and relative variation in tumor stiffness when compared with the surrounding, healthy tissue. More in-depth evaluation of these effects for prostate specimen tests is required to be carried out in future. The second limitation of this study is the small sample size, but herein we have adequately demonstrated that RMI is workable. The third limitation is that the prostate was lying on a flat and hard surface during application of the sensor probe. However, for in vivo tests there is a non-constant compliance for the application of this

sensor due to the surrounding anatomy, blood perfusion, muscle tension and pulsation, which could lead to artefacts. In addition, the robotic ports for MIS are 8 mm in size. The camera port in 12 mm in size and slightly extended to extract the specimen. One of the assistant ports is 12 mm in size. It is our eventual wish to be able to insert the RMI through the assistant port to guide the surgeon real time during MIS. This was a proof of concept study on freshly excised and extracted prostates in preparation for this future goal. The next phase will be to introduce the probe into robotic surgery in a phase I clinical trial.

6. References

[1] Megan M.M., Brian R.L.,Alwyn M.R., Ming Zhou, Cristina M-G, Eric A.K. Tumor Volume Does Not Predict for Biochemical Recurrence After Radical Prostatectomy in Patients with Surgical Gleason Score 6 or Less Prostate Cancer. Urology. 70(2):294-298 (2007)

[2] American Society of Colon and Rectal Surgeons: Minimally Invasive Surgery Expanded Version. https://www.fascrs.org/patients/disease-condition/minimally-invasive-surgery-expanded-version

[3] Dasgupta P., Jones A., Gill I.S. Robotic urological surgery: A perspective. BJU Int. 95. 20–23 (2005).

[4] Li, M., Liu, H., Jiang, A., Seneviratne, L. D., Dasgupta, P., Althoefer, K., Wurdemann, H. Intra-operative tumour localisation in robot-assisted minimally invasive surgery: A review. Proceedings of the Institution of Mechanical Engineers, Part H: Journal of Engineering in Medicine, Vol 228(5), pp 509-522, 2014

[5] Rifkin M. D., Zerhouni E. A., Gatsonis C. A., Quint L. E., Paushter D. M., Epstein J. I., et al, Comparison of magneticresonance imaging and ultrasonography in staging early prostate cancer. Results of a multi-institutional cooperative trial. N Engl J Med, 323–621(1990)

[6] Nakashima J, Tanimoto A, Imai Y,Mukai M and Horiguchi Y.,et al. Endorectal MRI for prediction of tumor site, tumor size, and local extension of prostate cancer. Urology 64(1):101-5(2004).

[7] Quint L.E., Van Erp J.S., Bland P.H., Mandell S.H., Del Buono E.A., Grossman H.B. et al. Carcinoma of the prostate: MR images obtained with body coils do not accurately reflect tumor volume, Am. J. Roentgenol, 156 511–516. (1991)

[8] Chelsky M.J., Schnall M.D., Fast spin-echo MR images of the pelvis obtained with a phased-array coil: value in localising and staging prostatic carcinoma, Am. J. Roentgenol., 161. 601–606(1993).

[9] Boni H., Boner J.A., Debatin J.F., Trinkler F., Knonagel H., Von Hochstetter A., et al. Optimisation of prostate carcinoma staging: comparison of imaging and clinical methods. Clin. Radiol., 50. 593–600.(1995)

[10]   Shinohara K, Wheeler T. M., Scardino P. T., The appearance of prostate cancer on transrectal ultrasonography: correlation of imaging and pathological examinations. J Urol, 142-76 (1989).

[11]   Choyke P.L., Imaging prostate cancer, Abdm. Imaging, 20. 505–515. (1995).

[12]   Lee F., Gray J. M., McLeary R. D., "Transrectal ultrasound in the diagnosis of prostate cancer: location, echogenicity, histopathology, and staging," Prostate, vol. 7. 117–129(1985).

[13]   Salomon G., Kolerman J., I.Thederan, Chun F, Budäus L, Schlomm T., Isbarn H, Heinzer H., Huland H., Graefen M.. Evaluation of prostate cancer detection with ultrasound real-time elastography: a comparison with step section pathological analysis after radical prostatectomy. European urology, 54, no. 6, 1354-1362 (2008).

[14]   Billings, S., Deshmukh, N., Kang, H. J., Taylor, R., & Boctor, E. M. System for robot-assisted real-time laparoscopic ultrasound elastography. In SPIE Medical Imaging (pp. 83161W-83161W). International Society for Optics and Photonics. (2012, February).

[15]   Correas J.M., Drakonakis E., Isidori A.M., Hélénon O., Pozza C., Cantisani V., Di Leo N. et al. Update on ultrasound elastography: Miscellanea. Prostate, testicle, musculo-skeletal. European journal of radiology 82, no. 11, 1904-1912 (2013)

[16]   Liu H., Noonan D. P., Challacombe B. J., Dasgupta P., Seneviratne L. D., Althoefer K., Rolling Mechanical Imaging for Tissue Abnormality Localization During Minimally Invasive Surgery. IEEE Trans. Biomed. Engineering 57(2): 404-414 (2010)

[17]   Liu H., Li J., Song X., Seneviratne L. D., Althoefer K., Rolling Indentation Probe for Tissue Abnormality Identification during Minimally Invasive Surgery. IEEE Transactions on Robotics 27(3): 450-460 (2011)

[18]   K Sangpradit, H Liu, P Dasgupta, K Althoefer, LD Seneviratne., Finite-element Modeling of Soft Tissue Rolling Indentation. IEEE Transactions on Biomedical Engineering 58 (12), 3319-3327(2011).

[19]   Y Noh, H Liu, S Sareh, DS Chathuranga, H Würdemann, K Rhode, K Althoefer., Image-based Optical Miniaturized Three-Axis Force Sensor for Cardiac Catheterization. IEEE Sensors Journal 16(22): 7924-7931(2016).

[20]   A Faragasso, A Stilli, J Bimbo, HA Wurdemann, K Althoefer. Multi-Axis Stiffness Sensing Device for Medical Palpation. In IEEE/RSJ In: IEEE international conference on Intelligent Robots and Systems (IROS):2711-2716 (2015)

[21]   A Faragasso, A Stilli, J Bimbo, Y Noh, H Liu, T Nanayakkara, P Dasgupta,HA Wurdemann, K Althoefer., Endoscopic add-on stiffness probe for real-time soft surface characterisation in MIS. In: the 36th Annual International Conference of the IEEE Engineering in Medicine and Biology Society (EMBC); 6517-20 (2014).

[22]   J Li, H Liu, K Althoefer and L D. Seneviratne., A Stiffness Probe Based on Force and Vision Sensing for Soft Tissue Diagnosis, In: 34th Annual International IEEE /EMBS Conference (EMBC):944-947(2012).

[23]   Miller A.P, Peine W.J, Son J.S, Hammoud Z.T. Tactile imaging system for localizing lung nodules during video assisted thoracoscopic surgery. In: IEEE international conference on robotics and automation (ICRA): 2996-3001 (2007).

[24]   Altman D, Bland J. Diagnostic test 1: sensitivity and specificity. BMJ 308: 1552 (1994)

[25]   Fawcett T. An introduction to ROC analysis. Pattern Recognit. Lett. 27:861–74(2006)

[26]   Wilson E. B. Probable inference. The law of succession and statistical inference J. Am. Stat. Assoc. 22: 209–12 (1927).

[27]   Y. C. Fung, Biomechanics: Mechanical Properties of Living Tissues.New York: Springer-Verlag, 1993, pp. 269–281.